EurJOC

European Journal of Organic Chemistry

Chemistry Europe

European Chemical Societies Publishing

Accepted Article

Title: Tandem Nenitzescu reaction/nucleophilic aromatic substitution to form novel pyrido fused indole frameworks

Authors: Rashmi Singh, Harshita Bhatia, Prabhat Prakash, Elke Debroye, Swapan Dey, and Wim Dehaen

To be cited as: *Eur. J. Org. Chem.* 10.1002/ejoc.202100827

Link to VoR: https://doi.org/10.1002/ejoc.202100827

WILEY-VCH

10.1002/ejoc.202100827

WILEY-VCH

FULL PAPER

Tandem Nenitzescu reaction/nucleophilic aromatic substitution to form novel pyrido fused indole frameworks

Rashmi Singh,[a,b] Harshita Bhatia,[c] Prabhat Prakash,[d] Elke Debroye,[c] Swapan Dey*[a] and Wim Dehaen*[b]

[a] Rashmi Singh, Dr. Swapan Dey
Department of Chemistry
Indian Institute of Technology (Indian School of Mines), Dhanbad
Dhanbad 826004, India.
E-mail: swapan@iitism.ac.in
URL: https://www.iitism.ac.in/~swapan
[b] Rashmi Singh, Prof. Wim Dehaen,
Molecular Design and Synthesis, Department of Chemistry,
KU Leuven.
Celestijnenlaan 200F, 3001 Leuven, Belgium.
E-mail: wim.dehaen@kuleuven.be
URL: https://chem.kuleuven.be/en/research/mds/losa/index.html
[c] Harshita Bhatia, Dr. Elke Debroye
Molecular Imaging and Photonics, Department of Chemistry,
KU Leuven.
Celestijnenlaan 200F, 3001 Leuven, Belgium.
[d] Dr. Prabhat Prakash
Materials Engineering,
Indian Institute of Technology Gandhinagar.
Palaj, Gandhinagar 382355, Gujarat, India.

Supporting information for this article is given via a link at the end of the document.

Abstract: 5-Hydroxyindoles are privileged structures that form part of various bioactive compounds. The Nenitzescu reaction of quinones and enamines is one of the most powerful methods to obtain 5-hydroxyindoles. In this work, we have applied the Nenitzescu reaction to 2-(2-chloropyrid-3-yl)benzoquinones. Mixtures of regioisomers were obtained that could be separated in the 4- and 6-substituted analogues, and then cyclized separately in a metal-free base-catalyzed reaction, affording novel tetracyclic indole derivatives. These are indeed the first examples reported in the literature of the linear pyrido[3',2':4,5]furo[3,2-*b*]indole and angular 1*H*-pyrido[2', 3':4,5]furo[2,3-*c*]indole systems. The regioselectivity and the yield of the Nenitzescu reaction were found to be dependent on the *N*-substituent at the enamine. Furthermore, we analysed the UV-Vis and PL spectra of the new systems, and this was supported by DFT calculations, allowing us to compare the properties of angular compared to linearly shaped compounds.

Introduction

"Privileged structure" is a term used in medicinal chemistry to define molecular frameworks like cyclic and polycyclic heteroatomic systems, capable of binding to multiple receptors as high-affinity ligands, yielding several biologically active compounds.[1–3] Quinones are strong electrophiles that can react in cyclocondensations with a wide array of nucleophiles to afford different polycyclic heterocycles, like the 5-hydroxyindoles and 5-hydroxybenzofurans (both processes are called the Nenitzescu reaction),[4–7] and many other heterocycles of medicinal interest. Polycyclic heterocycles are scaffolds present to a large extent in natural products and pharmaceuticals[8,9] and are characterized by a broad scope of activities.[10]

5-Hydroxyindole derivatives have been widely found in natural products[11] and biologically relevant compounds.[12] Serotonin (5-hydroxytryptamine) **1** is an important neurotransmitter in the central nervous system (CNS),[13,14] bufotenine **2**, a tryptophan-derived alkaloid is an anti-viral and antipsychotic agent.[11,15] Violacein **3** is a bisindole compound that has antibiotic activities,[16] while arbidol (ARB, also known as umifenovir) **4**, is a synthetic antiviral drug to combat the influenza virus.[17,18] LY311727 **5** has been described as a selective inhibitor of human nonpancreatic s-PLA_2, and the ether derivative indomethacin **6**, a non-steroidal drug, has been used as an anti-inflammatory agent.[19,20] The N-(4-fuorobenzyl)indole derivative AWD 12- 281 **7** is a potent and selective PDE-4 inhibitor that has been used as an anti-inflammatory agent in the treatment of asthma (Figure 1).[1]

Indole-fused, further extended poly-heterocycles are also of great importance in drug design and discovery.[21–27] It is noteworthy that compounds with a pyrido furo fused skeleton possess remarkable bioactivities including, analgesic, anti-inflammatory, anti-proliferative,[28][29] anti-microbial and anti-allergic activity.[30,31] Other features can be referred to as dual endothelin receptor (ETA and ETB) antagonist,[32] selective GSK-β inhibitor important in Alzheimer disease.[33,34] In this context, efficient synthetic strategies towards the construction of challenging hybrid molecule with these two heterocycles pyridine, furan and additional indoles as key components have received great attention. One example is Revamilast **8**, a benzofuropyridine derivative (Figure 2), that has been used for the treatment of inflammatory disorders including rheumatoid arthritis .[35] Another representative **9** was reported to possess pronounced antibacterial activity against mycobacteria. 7,8-

Dimethoxybenzofuro[3,2-*b*]quinoline-2-ol **10** is a potent inhibitor of type I topoisomerase enzyme and has been used as an anti-tumor agent.[36] A literature survey indicates that several synthetic approaches have been reported for the construction of related fused indole[37–40] and benzofuropyridine containing frameworks.[41–45] The representative strategies used to construct these framework are based on cascade reactions,[46] organocatalyzed reactions,[47][48] palladium catalysed couplings [49], and post-Ugi transformations.[50] Langer and co-workers reported the palladium mediated synthesis of benzofuropyridines using nitro-substituted heteroarenes as a substrate for further C-H activation.[51] Later, the same research group reported an alternative route using a domino protocol of 3-chlorochromones with amino heterocycles. The synthesis of benzofuropyridines has been recently reported by our group via Meerwein arylation of 1,4-benzoquinone with 3-amino-2-chloropyridines.[52] Among the many procedures reported, the Nenitzescu indole synthesis has proved to be the simplest and efficient strategy for obtaining 5-hydroxyindole analogs directly and/or selectively starting from easily accessible synthons. In the framework of an ongoing interest in Nenitzescu condensation to generate 5-hydroxyindole,[4,5,53] we have been exploring this approach in combination with the Meerwein approach towards the synthesis of pyrrole-fused benzofuropyridine derivatives starting from easily accessible starting materials like quinones and enamines. To the best of our knowledge the direct synthesis of such scaffolds based on a Nenitzescu approach is not yet reported.

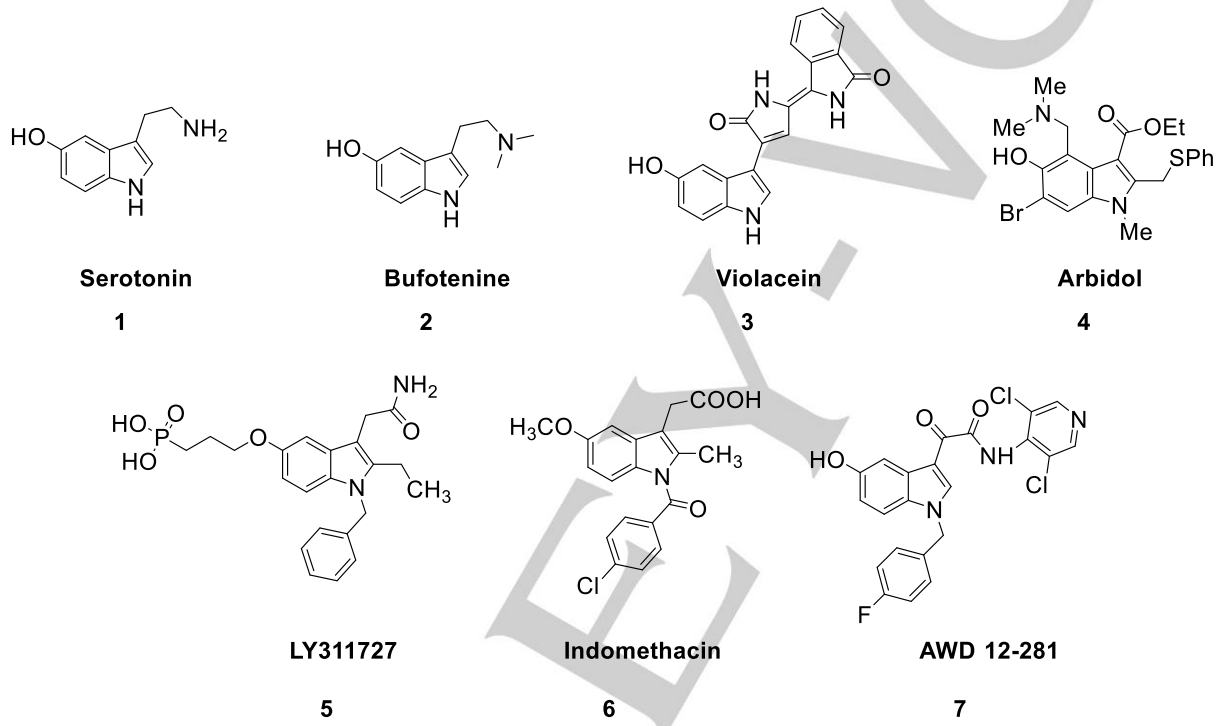

Figure 1. Natural and synthetic biologically active compounds containing 5-hydroxyindole nucleus **1-7**.

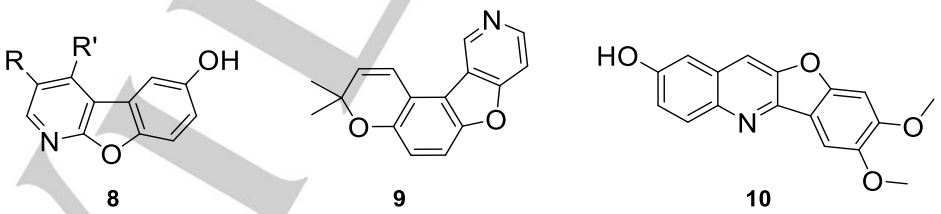

Figure 2. Representative bioactive analogues of benzofuropyridines **8**-**10**.

Here, we report our efforts to prepare various *N*-substituted 5-hydroxy indoles *via* the Nenitzescu condensation. The Nenitzescu product was easily transformed by intramolecular nucleophilic aromatic substitution into the novel angularly and linearly pyrido (furo) fused indole frameworks which are core structures of several bioactive compounds. The formation of these hybrid molecular scaffolds with indole, pyridine and furan moieties is highly noteworthy as the reported methods for the synthesis of fused indoles often require multi-step synthesis and harsh conditions. Furthermore, this strategy provides simple straightforward access to these frameworks from easily available starting materials under mild conditions. We also report the photophysical properties of the pyrido (furo) indole derivatives.

Results and Discussion

Synthesis and characterization:

The target compound **14 (**or its isomer **15)** was synthesized in a two-step process utilizing the synthetic route summarised in Scheme 1. The arylquinone **11** used in this study was prepared as recently reported in our work related to the synthesis of benzofuropyridines via the Meerwein arylation followed by reductive cyclization.[52] The enamines **12** were prepared by following a literature procedure.[54] The first step is the Michael addition of the β-carbon of the enamine **12a** to 2-(2-chloropyridin-3-yl)cyclohexa-2,5-diene-1,4-dione **11**, followed by a cyclocondensation and loss of water. The Nenitzescu adduct **13a** and its isomer **13'a**, precursors to the synthesis of the target compounds, were obtained by the condensation of commercially available ethyl-3-aminocrotonate **12a** with the 2-(2-chloropyridin-3-yl)cyclohexa-2,5-diene-1,4-dione **11**.

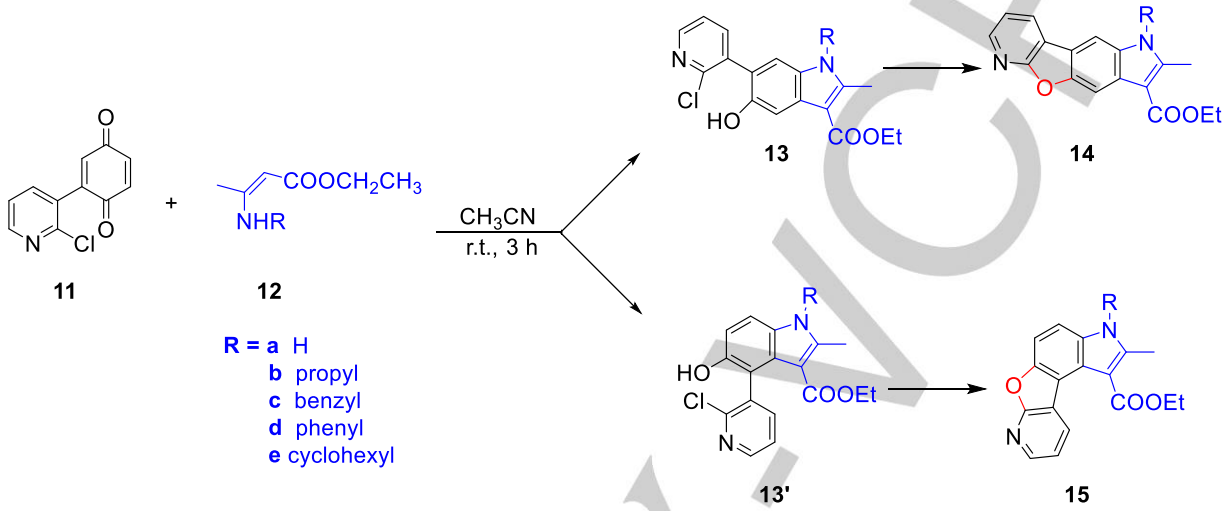

Scheme 1. Synthetic strategies for the pyrido (furo) fused indoles.

Initially, we optimised the reaction of enamines **12** and quinone **11**. Adding enamine **12a** into a solution of 2-(2-chloropyridin-3-yl)cyclohexa-2,5-diene-1,4-dione **11** in acetonitrile at room temperature led to a mixture of two regioisomers, **13a** and **13'a** namely, C6 and C4 substituted Nenitzescu adducts respectively in a 1:1.6 ratio and these were separated by chromatography in 30% and 50% yield respectively along with the isolation of 8% of the uncyclized hydroquinone derivative of starting material **11.**[52] Despite the formed mixture of regioisomers and the low regioselectivity, we could separate the two isomeric products. Following this, each isomer was carried forward in the synthetic route. The structure of both the regioisomers was unambiguously confirmed by ^{1}H and ^{13}C NMR spectroscopy, and HRMS. An examination of their ^{1}H NMR spectrum revealed that these were indeed the desired **13a** and **13'a**. The ^{1}H spectra of **13'a**, in contrast to the spectra of the **13a**, shows the diastereotopic splitting of the signals corresponding to the -CH_2 group and these are seen as two doublets of quartets at δ_H 3.5 (dq, J = 10.8 Hz, 1H) and δ_H 3.65 (dq, J = 10.8 Hz, 1H) proving it is a 4-substituted derivative. In fact, all the Nenitzescu adducts were obtained as atropoisomer mixtures. In the case of 6-substituted **13a**, two distinct singlets at δ_H 8.10 (H-4) and δ_H 8.13 (H-7) are observed which confirm that the pyridine ring is attached to the C6 position of the indole ring. In the case of 4-substituted isomer **13'a**, two separate doublet signals at δ_H 6.81 (d, J = 8.6 Hz, 1H) and δ_H 7.25 (d, J = 8.5 Hz, 1H) confirm the addition of the pyridine ring to the C4 position of the indole ring.

In order to optimize the best result, we screened a small set of different solvents such as acetic acid, ethanol, nitromethane. We also explored the influence of Lewis acid on the outcome of the Nenitzescu reaction. In particular, we tried a reaction of 2-(2-chloropyridin-3-yl)cyclohexa-2,5-diene-1,4-dione **11** with 1.2 equiv. of **12a** using 1 mol% zinc iodide in CH_2Cl_2 at 40 ºC for 2 h.[55] The yield did not improve for the reaction with the use of Lewis acid, even after increasing the reaction time. Although the reaction proceeded in all the solvents, there was no considerable improvement of the yield and regioselectivity of the reaction. In some cases, even the conversion of the reactant was significantly decreased. Therefore, the optimised conditions for the synthesis of Nenitzescu adducts involved treatment of 1 equiv. of 2-(2-chloropyridin-3-yl)cyclohexa-2,5-diene-1,4-dione **11** with 1 equiv. of enamine **12a** in acetonitrile under air at room temperature for 3 h.

Next, for the substrate scope exploration, several substituted enamines **12b-e** were subjected to our optimised reaction conditions. We varied the substituent at the nitrogen of the enamines with both primary aliphatic and aromatic groups. Remarkably, an improved ratio favouring the C4 substituted isomer was observed. On switching towards the primary acyclic group as for the propyl substituted **12b**, the reaction worked efficiently under standard conditions to afford a mixture of two regioisomers **13b** and **13'b** in 7% and 43% yield, respectively (Table 1). Similarly, for benzylic *N*-substituted **12c**, a mixture of **13c** and **13'c** in 11% and 74% isolated yield, respectively was obtained. In both cases, the ratio of the required isomers in the crude mixtures was similar i.e. 1:6 and the C6 Nenitzescu adducts were isolated as a minor product.

We then introduced the phenyl substituent at the nitrogen of the enamine. Enamine **12d** led to the formation of the two regioisomers **13d** and **13'd** in a 1:4 ratio, in a poor 2% and 8% isolated yield, respectively. The low isolated yield of the reaction could be explained by (1) the lower reactivity of *N*-aryl enamines (2) the formation of a significant amount of highly coloured impurities and oligomers (3) production of by-products (reduced

hydroquinone corresponding to the benzoquinone **11** used) causing difficulties during the column chromatography purification of the isomers.

Table 1. Scope of the reaction with respect to enamines **12a**-**e**.

11	enamine **12b-e**	Nenitzescu adduct		ratio
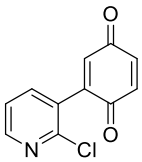	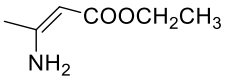 **12a**	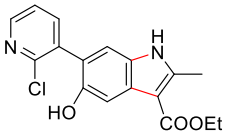 **13a** (30%)	+ 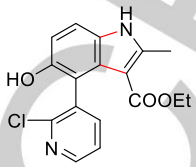 **13'a** (50%)	1:1.67
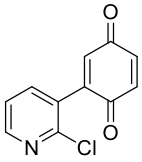	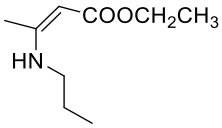 **12b**	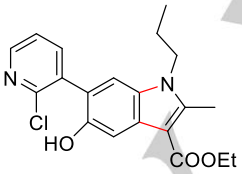 **13b** (7%)	+ 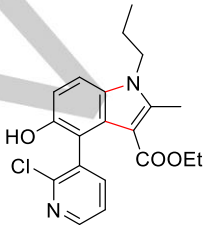 **13'b** (43%)	1:6.33
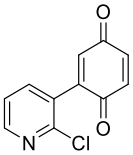	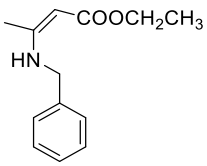 **12c**	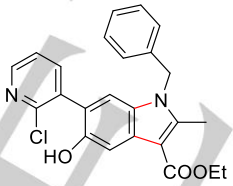 **13c** (11%)	+ 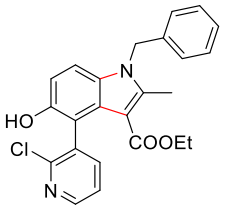 **13'c** (74%)	1:6.21
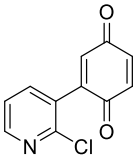	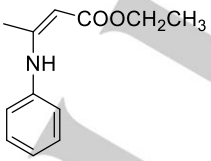 **12d**	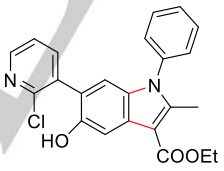 **13d** (2%)	+ 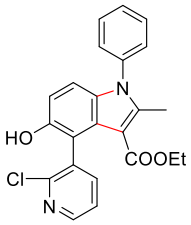 **13'd** (8%)	1:5
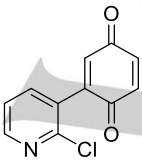	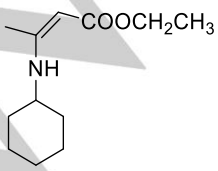 **12e**	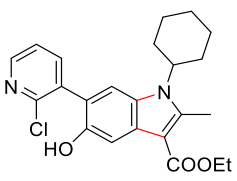 **13e**	+ 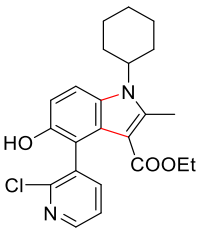 **13'e**	-

Next, we varied to cyclohexylamine as a cyclic primary aliphatic amine. Unfortunately, we could observe (TLC) only traces of the desired product, obtained complex mixtures and observed poor conversion of the reactant.

If we summarise the result of this small scope investigation, it can be stated that the *N*-substitution indeed improved the regioselective formation of the 4-substituted isomer. The decrease in the yield for aniline and cyclohexylamine could be attributed to steric and electronic reasons. The reaction was found to give only traces of product when a bulky cyclohexyl substituent is present on the nitrogen of the enamine. The aliphatic *N*-substituted enamines gave better yield than the less nucleophilic *N*-aromatic enamines.

Despite having regioselectivity issues, with easy access to thus obtained isomeric Nenitzescu adducts **13a-13'a**, we proceeded further to examine the cyclization to obtain polyfused ring systems.[42] The presence of the hydroxyl and chloro groups in the adducts **13a** and **13'a** allows us to study the subsequent intramolecular cyclization. The 5-hydroxyindole **13a** (or isomer **13'a**) could undergo an intramolecular nucleophilic attack involving the formation of a C-O bond, to lead to the corresponding polycyclic pyrido (furo) fused indole **14a** (or **15a**). Initially, we screened solvents such as DMSO and DMF with KOtBu base. The reaction failed to deliver the required product **14a** as the ester part of the pyrrole ring was hydrolysed, probably due to traces of water present. Next, other bases such as K_2CO_3 and NaOEt were screened in DMF and ethanol solvent. The use of K_2CO_3 in DMF under refluxing conditions conveniently gave the best result. The intermediate **13a** and **13'a** afforded the desired cyclized product **14a** and **15a** in 83% and 89% isolated yield, respectively within 2 h. The formation of synthesized compounds **14a** and **15a** was confirmed by ^{1}H NMR spectroscopy. The compound **14a** displayed two characteristic singlets separately at δ_H 8.09 and δ_H 8.12 which confirmed the 5,6-disubstituted indole pattern. The substitution of the chloro group caused an upfield shift of the resonance signal concerning the pyridine part. On the other hand, the ^{1}H NMR spectra of compound **15a** revealed two separate doublet signals at δ_H 7.62 (d, J = 8.7 Hz, 1H) and δ_H 7.57 (d, J = 8.8 Hz, 1H) indicating an *ortho*-relationship between the 6,7-hydrogens positioned onto the indole ring. Overall, this synthesis is interesting because the reaction provides a concise and mild route to variously substituted pyrido (furo) fused indoles that have not been previously obtained. Similarly, angularly and linearly fused polyheterocycles **14(a-c) and 15(a-c)** could be conveniently synthesized, in fair to excellent yield under similar conditions to compound **14a**. (Scheme 2).

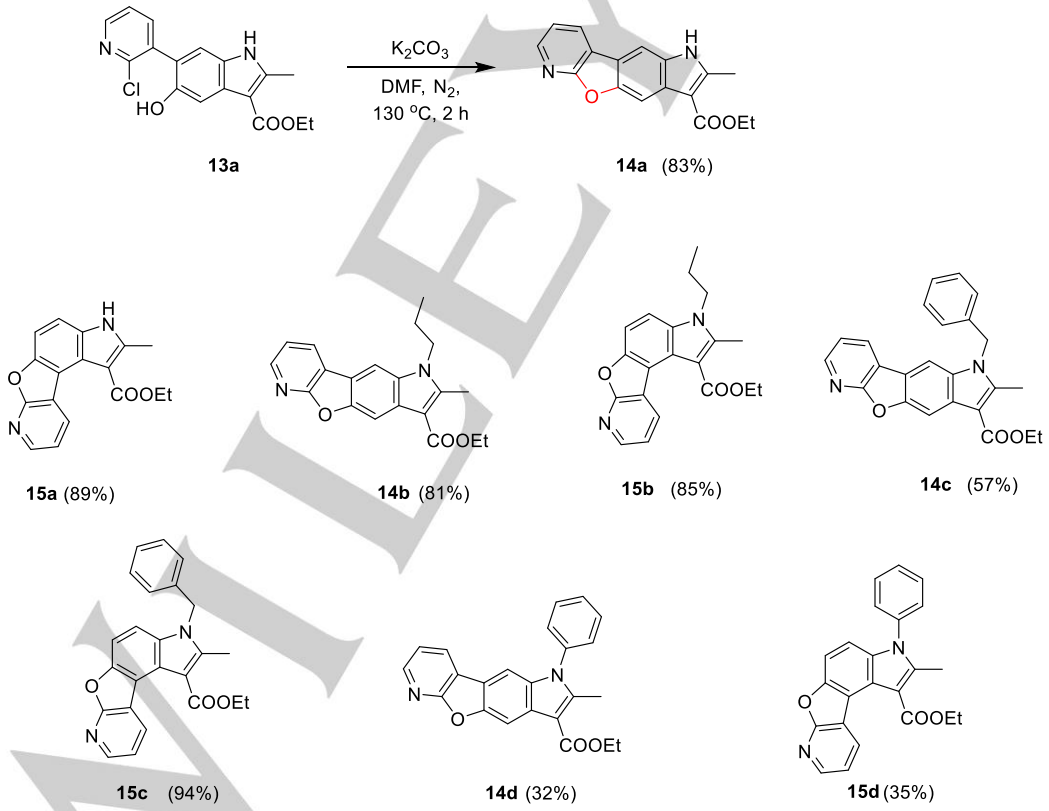

Scheme 2. Synthesis of various examples of pyrido (furo) fused indole **14** and **15**.

Spectroscopic properties:

The UV-Vis absorption and photoluminescence (PL) spectra of all the synthesized compounds were recorded in solvents of different polarities: acetonitrile and toluene. The normalized spectra for **15a** and **14b** are shown in Figure 3, those for **15b, 14c** and **15c** are provided in the Supporting information Figure S1. The values of the wavelength with maximum emission intensity, the Stokes shift, and full width at half maximum (FWHM) of the emission peak

(FWHM) from these spectra and their comparison with DFT calculations (discussed *vide infra*) are provided in **Table 2.** All these compounds exhibit an absorption maximum, $\lambda_{abs,}$ from 329 – 343 nm, and an emission maximum, $\lambda_{em,}$ from 362 – 395 nm, with a Stokes shift of 3400 – 4200 cm^{-1} in acetonitrile, and ~ 2500 cm^{-1} in toluene. In the absorption spectra of **15a, 15b** and **15c**, two vibronic bands of almost equal intensities, centred at around 329 – 348 nm and 318 – 326 nm, are assigned to the transitions from S0 – S1. However, in the absorption spectra of **14b** and **14c**, there is a difference in the relative intensity of the secondary peak, which could be attributed to the geometrical difference of linear *vs.* angular. In general, the absorption spectra of all the compounds are hardly affected by the solvent polarity; a slight hypsochromic shift of about 7 nm is observed when the solvent is changed from toluene to acetonitrile, owing to the low polarizability of acetonitrile. This also suggests a slight change in the dipole moment of these compounds with respect to the solvent (Table S3). Furthermore, the shape of the absorption and PL excitation spectra in both solvents is shown to coincide reasonably well (Figure S2).

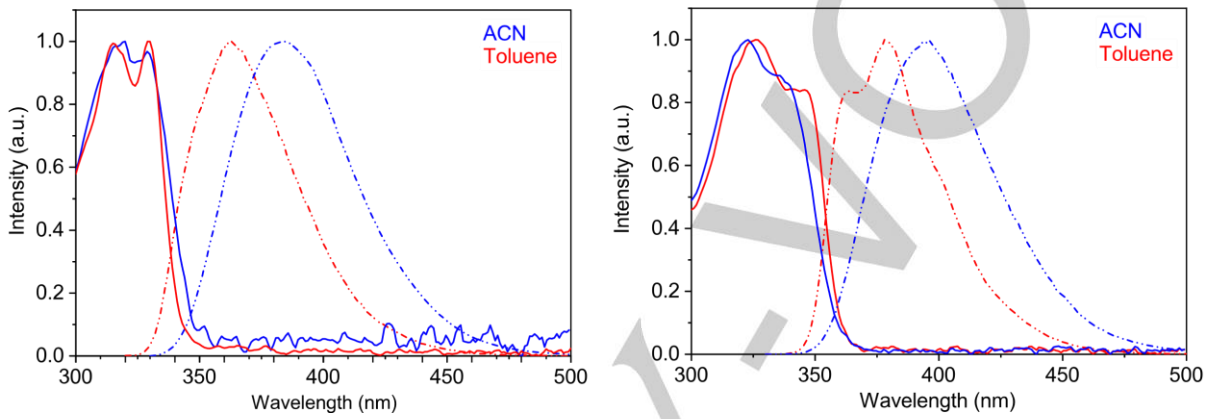

Figure 3. UV-Vis absorption (solid line) and PL emission (dashed line) spectra of compound **15a** (left) and **14b** (right) in acetonitrile (blue) and toluene (red).

The solvent dependence of PL emission in these compounds is fairly interesting. The fluorescence bands broaden and shift bathochromically with increasing solvent polarity (from 363 nm for toluene to 395 nm for acetonitrile). Moreover, the shape of the emission spectra also differs on varying the polarity of the solvents. Specifically, the PL spectra of **14b** and **14c** in toluene are vibronically structured, whereas only a shoulder peak is observed for **15(a-c)**, indicating that the emission originates from the localized energy states. However in acetonitrile, only one broad band at a higher wavelength region could be discerned, implying the formation of a charge-transfer state as the solvent polarity increases.[56,57] This solvatochromism is attributed to solvent relaxation, leading to charge transfer due to the high polarity of acetonitrile compared to toluene. Additionally, the solvatochromism of **15b** and **15c** was also tested with dimethylsulfoxide (DMSO) and methanol (MeOH) solvents (Figure S3), which showed only a slight change in λ_{abs} and a moderate red shift in λ_{em} values (Table S1) when compared to acetonitrile.

Notably, the photoluminescence quantum yield (ϕ) for all the compounds increases with the decrease in solvent polarity. However, there is only a slight difference in the values of ϕ, ranging from 65 – 83% at 310 nm excitation. This depicts that the influence of the solvent on the PLQY of these compounds is minimal (Table 2). Furthermore, the FWHM of all the derivatives is narrower than that of the unsubstituted one (**15a**), and is also found to increase with the increase in the solvent polarity, varying between 3416 cm^{-1} in toluene and 3963 cm^{-1} in acetonitrile.

The theoretical simulation of absorption and emission spectra were performed with time-dependent-density functional theory (TD-DFT) calculations for **15a, 14b, 15b, 14c and 15c** under continuum solvation environment for both the solvents using B3LYP/6-31+G(d,p) method on Gaussian 09 Rev. D01 software package.[58] The calculated values of λ_{max}, for absorption (calculated from a ground state stationary point), and emission (calculated from an excited state optimized geometry predicted from TD-DFT) are provided in Table 2 for validation and comparison. The DFT results show a close agreement with the respective λ_{max} values observed from the experiments ($|\lambda_{exp} - \lambda_{DFT}| < 5\%$ for all absorption and emission values).

To understand the effect of linear *vs.* angular geometry and solvent polarity on the absorption and emission spectra, frontier orbitals of all the compounds were analyzed for the ground state geometries with a polarized continuum solvation model for acetonitrile. The relative energies and electron densities on the HOMO and LUMO orbitals are presented in Figure 4. The wavelengths associated with the electronic energy gap between the HOMO and LUMO are annotated with arrows in Figure 4. The calculated wavelengths are: ~ 292 nm for **15(a-c)**, and ~ 300 nm for **14b** and **14c**. The difference (292 nm and 300 nm) of these pure electronic gaps is ~ 8 nm, which is similar to the difference in $\lambda_{max,abs}$ from UV-Vis spectra. Further, the geometrical arrangement of these compounds also affects the electron density distribution for HOMO and LUMO. The linear molecular geometry of **14b** and **14c** compared to the angular geometry of **15(a-c)** results in two particular differences in the UV-Vis and PL spectra: i) slightly red-shifted absorption and emission lines for **14b** and **14c** compared to **15(a-c)**; ii) the presence of a low-intensity secondary absorption peak for **14b** and **14c**, compared to two equal intensity peaks in **15(a-c)**. For **15(a-c)**, the lobe of the longest conjugation also appears above/close to the oxygen atom of the furan ring, which is contrasting to a localized *p*-orbital

kind of density present on the O atom in **14b** and **14c**. This difference manifests in a broader absorption spectrum for **14b** and **14c** irrespective of solvent. To provide the quantitative understanding of geometrical changes in the ground and excited states of the compounds, dipole moments were also calculated and are provided in the Supporting Information Table S2. The calculated dipole moments for ground-state geometries of linear **14b** and **14c** are slightly larger compared to the angular **15(a-c)**.

Finally, simulated UV-Vis spectra for all these compounds were calculated using six excited states in the TD-DFT framework (Figure S4 in the Supporting Information). The simulated absorption spectra exhibit two different shapes of absorption spectra which inherently affirm the two more resolved peaks for the angular compounds **15(a-c)** compared to a slightly low-intensity secondary peak for the linear **14b** and **14c**.

Table 2. UV-Vis absorption and fluorescence emission spectroscopic data for **15a, 14b, 15b, 14c** and **15c** in the solvents: acetonitrile and toluene. Subscripts: abs = absorption, em = emission, exp. = from experiments; $\bar{\nu}$ = Stokes Shift, **ε** = molar absorptivity.

Entry	Solvent	$\lambda_{abs,exp}$ (nm)	$\lambda_{abs,DFT}$ (nm)	$\lambda_{em,exp}$ (nm)	$\lambda_{em,DFT}$ (nm)	FWHM $_{em,exp}$ (cm^{-1})	$\bar{\nu}_{exp}$ (cm^{-1})	f_{DFT}	ϕ_{exp} (%)	ε ($mol\text{-}L^{-1}\text{-}cm^{-1}$)
15a	ACN	329	323	384	379	3952	4353	0.6723	73	15441 ± 52
	Tol	330	317	362	358	3729	2679	0.5175	78	19333 ± 140
14b	ACN	338	339	395	388	3553	4269	0.7891	72	23600 ± 390
	Tol	342	339	378	372	3416	2785	0.4944	83	26600 ± 570
15b	ACN	332	323	390	379	3963	4479	0.6827	70	21721 ± 1100
	Tol	335	317	370	368	3735	2823	0.5269	75	16300 ± 230
14c	ACN	336	341	390	407	3756	4121	0.7914	73	15500 ± 450
	Tol	343	336	376	379	3614	2416	0.4820	80	28000± 380
15c	ACN	332	333	383	393	3836	4078	0.6657	65	31700 ± 200
	Tol	334	331	366	376	3494	2617	0.4993	80	24300 ± 500

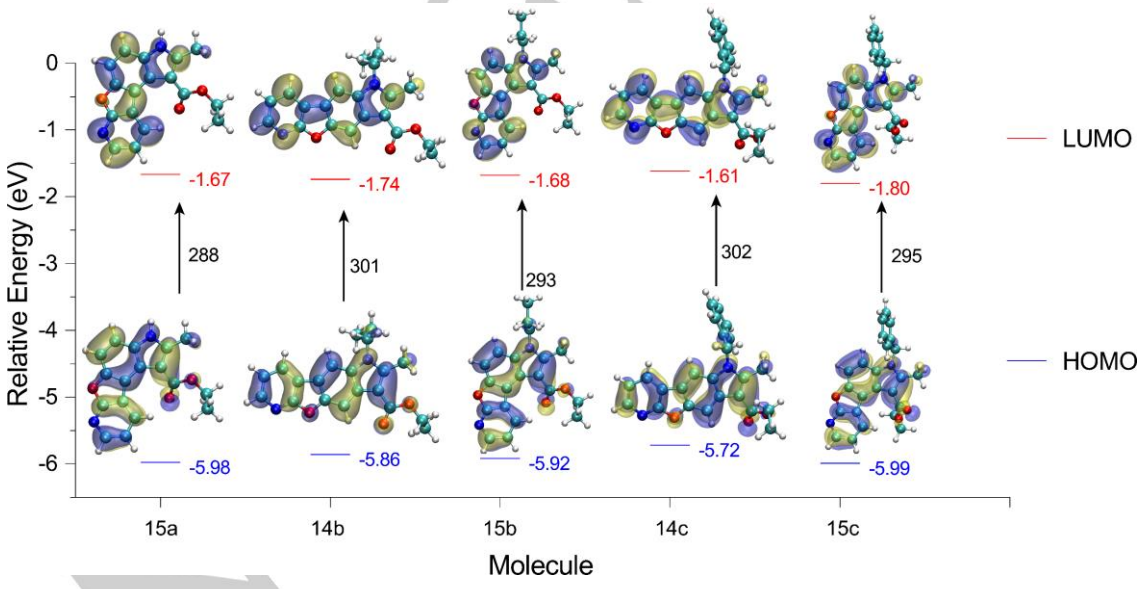

Figure 4. HOMO and LUMO for compounds **15(a,b** and **c), 14b** and **14c** with their relative energies calculated for ground state optimized geometries using B3LYP/6-31+G(d,p) in acetonitrile. Energies (eV) for the HOMO are annotated in blue, and for the LUMO in red. The wavelengths (nm) corresponding to the HOMO – LUMO gap in each case are annotated in black tight next to the arrow.

Conclusion

In conclusion, a straightforward approach to synthesize a diverse range of the desired Nenitzescu adducts of 2-(2-chloropyridin-3-yl)cyclohexa-2,5-diene-1,4-dione **11** and enamines **12a-e**

derivatives has been developed. This method requires only inexpensive or readily available reagents and works under simple reaction conditions at room temperature. Furthermore, the hydroxyl group in the prepared isomeric adducts **13a-13d** undergoes an intramolecular nucleophilic aromatic substitution potentially leading to the novel ring-closed products **14** and **15**, a new class of fused indole-derivatives, under mild conditions in excellent yields. Our strategy provides an alternative to literature methods where usually a metal-catalyzed approach has been utilized. This finding provides new access to various pharmacologically interesting pyrido (furo) fused indole motifs in a highly concise fashion. The optical properties of synthesized ring-closed compounds were analyzed using UV-Vis and PL spectra. The DFT calculations provide a molecular orbital and geometrical basis for the effect of solvent polarity, Stokes shift and slightly blue-shifted peaks for angular compared to linear shaped compounds.

Experimental Section

General Information: Chemicals received from commercial sources (Sigma-Aldrich, Acros Organics, J&K Scientific, Alfa Aesar or TCI Chemicals) were used without further purification. Column Chromatography was performed over Acros silica gel (60 Å). Dry reaction solvents were purchased from commercial sources. Thin-layer chromatography (TLC) was performed on silica gel 0.20 mm 60 with fluorescent indicator UV254 (pre-coated aluminum sheets) from Merck. For column chromatography 60-200 mesh silica gel 60 (Acros) was used as stationary phase. NMR spectra were acquired on commercial instruments (Bruker Avance 300 MHz, Bruker AMX 400 MHz or Bruker Avance II$^+$ 600 MHz) and chemical shifts (δ) are reported in parts per million (ppm) referenced to tetramethylsilane (^{1}H), or the internal (NMR) solvent signal (^{13}C). High resolution mass spectra were acquired on a quadrupole orthogonal acceleration time-of-flight mass spectrometer (Synapt G2 HDMS, Waters, Milford, MA, USA). Samples were infused at 3µL/min and spectra were obtained in positive mode with a resolution of 15 000 (FWHM) using leucine enkephalin as lock mass. Melting points (uncorrected) were determined using a Reichert Thermovar apparatus. IR spectra were recorded on a Bruker Vertex 70 ATR-FTIR spectrophotometer.

General procedure for the synthesis of Enamines (12b-d)[54]**:** To a solution of ethyl acetoacetate (1 mmol) in acetonitrile (6 mL) was added various amines (1.2 mmol) and iodine (0.1 mmol). The mixture was placed at room temperature for vigorous stirring. The resulting 3-aminocrotonates have been purified by column chromatography and involved in Nenitzesu indole synthesis.

Characterisation of some representative enamines:

Ethyl (Z)-3-(propylamino)but-2-enoate (12b): Yellow oily liquid (150 mg, 95%). **^{1}H NMR** (400 MHz, $CDCl_3$) δ 8.55 (s, 1H), 4.40 (s, 1H), 4.05 (q, *J* = 5.3 Hz, 2H), 3.16 – 3.11 (m, 2H), 1.88 (s, 3H), 1.56 (h, *J* = 7.3 Hz, 2H), 1.21 (t, *J* = 7.1 Hz, 3H), 0.94 (t, *J* = 7.4 Hz, 3H). **^{13}C NMR** (101 MHz, $CDCl_3$) δ 170.73, 162.04, 81.83, 58.26, 44.81, 23.73, 19.42, 14.72, 11.42. **HRMS** (ESI+): *m/z* calculated for $C_9H_{17}NO_2$ $[M+H]^+$: 172.1332, found 172.1344.

Ethyl (Z)-3-(benzylamino)but-2-enoate (12c): Yellow oily liquid (376 mg, 93%). **^{1}H NMR** (400 MHz, $CDCl_3$) δ 8.95 (s, 1H), 7.35 – 7.31 (m, 2H), 7.27 – 7.23 (m, 3H), 4.53 (s, 1H), 4.41 (d, *J* = 6.4 Hz, 2H), 4.09 (q, *J* = 7.1 Hz, 2H), 1.90 (s, 3H), 1.25 (t, *J* = 7.1 Hz, 3H). **^{13}C NMR** (101 MHz, $CDCl_3$) δ 170.64, 161.86, 138.81, 128.83, 127.39, 126.76, 83.24, 58.43, 46.83, 19.41, 14.69. **HRMS** (ESI+): *m/z* calculated for $C_{13}H_{17}NO_2$ $[M+H]^+$: 220.1332, found 220.1331.

Ethyl (Z)-3-(phenylamino)but-2-enoate (12d): Yellow oily liquid (370 mg, 84%). **^{1}H NMR** (400 MHz, $CDCl_3$) δ 10.44 (s, 1H), 7.34 – 7.29 (m, 2H), 7.16 – 7.12 (m, 1H), 7.11 – 7.05 (m, 2H), 4.71 (s, 1H), 4.16 (q, *J* = 7.1 Hz, 2H), 1.99 (s, 3H), 1.29 (t, *J* = 7.1 Hz, 3H). **^{13}C NMR** (101 MHz, $CDCl_3$) δ 170.31, 158.79, 139.30, 128.99, 124.81, 124.27, 86.07, 77.48, 77.16, 76.84, 58.64, 20.19, 14.53. **HRMS** (ESI+): *m/z* calculated for $C_{12}H_{15}NO_2$ $[M+H]^+$: 206.1175, found 206.1179.

Ethyl (Z)-3-(cyclohexylamino)but-2-enoate (12e): Yellow oily liquid (365 mg, 94%). **^{1}H NMR** (400 MHz, $CDCl_3$) δ 8.61 (s, 1H), 4.36 (s, 1H), 4.06 (q, *J* = 7.1 Hz, 2H), 3.33 – 3.23 (m, 1H), 1.91 (s, 3H), 1.85 (dt, *J* = 6.7, 3.8 Hz, 2H), 1.76 – 1.70 (m, 2H), 1.59 – 1.53 (m, 1H), 1.33 – 1.25 (m, 4H), 1.22 (t, *J* = 7.1 Hz, 4H). **^{13}C NMR** (101 MHz, $CDCl_3$) δ 170.69, 160.90, 81.74, 77.48, 77.16, 76.84, 58.23, 51.51, 34.38, 25.48, 24.77, 19.31, 14.77. **HRMS** (ESI+): *m/z* calculated for $C_{12}H_{21}NO_2$ $[M+H]^+$: 212.1645, found 212.1649.

General procedures for the synthesis of Ethyl 5-Hydroxyindolecarboxylates (13a, 13'a, 13b, 13'b, 13c, 13'c, 13d, 13'd): To a solution of enamine **12a** (1.52 µl, 1.55 mmol) in acetonitrile (3 ml) was added 2-(2-Chloropyridin-3-yl)cyclohexa-2,5-diene-1,4-dione **11** (340 mg, 1.55 mmol) portion wise. The mixture was placed at room temperature for vigorous stirring for 3 h. The completion of the reaction was monitored by the TLC. The acetonitrile was concentrated and crude was purified by the column chromatography.

Ethyl 6-(2-chloropyridin-3-yl)-5-hydroxy-2-methyl-1*H*-indole-3-carboxylate (13a): Brown solid (154 mg, 30%). **Mp** 290 – 292˚C; **^{1}H NMR** (400 MHz, DMSO) δ 12.15 (s, 1H), 8.62 (dd, *J* = 7.5, 2.0 Hz, 1H), 8.37 (dd, *J* = 5, 1.8 Hz, 1H), 8.13 (s, 1H), 8.10 (s, 1H), 7.46 (dd, *J* = 7.5, 4.7 Hz, 1H), 4.33 (q, *J* = 7.1 Hz, 2H), 2.72 (s, 3H), 1.40 (t, *J* = 7.1 Hz, 3H). **^{13}C NMR** (101 MHz, DMSO) δ 164.86, 163.02, 150.12, 147.37, 145.29, 132.05, 129.98, 127.91, 119.18, 117.33, 117.27, 103.81, 102.98, 101.55, 58.98, 14.49, 14.09. **HRMS** (ESI+): *m/z* calculated for $C_{17}H_{15}ClN_2O_3$ $[M+H]^+$: 331.0844, found 331.0845. **IR:** 3066, 2976, 2927, 2900, 1682, 1480, 1186, 1158, 1083, 1036,1000, 980, 882, 794, 783, 772, 755, 741, 622 cm^{-1}.

Ethyl 4-(2-chloropyridin-3-yl)-5-hydroxy-2-methyl-1*H*-indole-3-carboxylate (13'a): Brown solid (256 mg, 50%). **Mp** 200 – 202 ˚C; **^{1}H NMR** (400 MHz, DMSO) δ 11.63 (s, 1H), 8.86 (s, 1H), 8.30 (dd, *J* = 4.7, 2 Hz, 1H), 7.56 (dd, *J* = 7.5, 2.0 Hz, 1H), 7.36 (dd, *J* = 7.5, 4.8 Hz, 1H), 7.25 (d, *J* = 8.6 Hz, 1H), 6.82 (d, *J* = 8.6 Hz, 1H), 3.65 (dq, *J* = 10.8, 7.1 Hz, 1H), 3.50 (dq, *J* = 10.8, 7.1 Hz, 1H), 2.51 (s, 3H), 0.92 (t, *J* = 7.1 Hz, 3H). **^{13}C NMR** (101 MHz, DMSO) δ 164.48, 150.92, 149.31, 146.93, 143.98, 140.52, 135.18, 129.40, 125.16, 122.14, 114.46, 112.04, 111.30, 104.06, 79.20, 58.50, 14.10, 14.02. **HRMS** (ESI+): *m/z* calculated for $C_{17}H_{15}ClN_2O_3$ $[M+H]^+$: 331.0844, found 331.0847. **IR:** 3436, 2250, 2124, 1673, 1427, 1393, 1175, 1053, 1024, 1005, 820, 758, 623 cm^{-1}.

Ethyl 6-(2-chloropyridin-3-yl)-5-hydroxy-2-methyl-1-propyl-1*H*-indole-3-carboxylate (13b): White solid (91 mg, 7%). **Mp** 165 – 167 ˚C; **^{1}H NMR** (400 MHz, $CDCl_3$) δ 8.42 (dd, *J* = 4.7, 2.0 Hz, 1H), 7.79 (dd, *J* = 7.5, 2.0 Hz, 1H), 7.76 (s, 1H), 7.33 (dd, *J* = 7.5, 4.8 Hz, 1H), 7.12 (s, 1H), 4.38 (q, *J* = 7.1 Hz, 2H), 4.04 (t, *J* = 7.4 Hz, 2H), 2.76 (s, 3H), 1.79 (h, *J* = 7.4 Hz, 2H), 1.42 (t, *J* = 7.1 Hz, 3H), 0.96 (t, *J* = 7.4 Hz, 3H). **^{13}C NMR** (101 MHz, $CDCl_3$) δ 166.37, 151.44, 148.91, 148.51, 146.23, 141.28, 134.61, 131.01, 128.48, 122.36, 120.45, 111.42, 107.45, 103.64, 77.48, 77.16, 76.84, 65.98, 59.70, 45.13, 23.24, 15.36, 14.76, 12.29, 11.51. **HRMS** (ESI+): *m/z* calculated for $C_{20}H_{21}ClN_2O_3$ $[M+H]^+$: 373.1313, found 373.1303. **IR:** 3282, 2978, 2933, 2877, 1645, 1629, 1583, 1557, 1510, 1456, 1447, 1428, 1396,1378, 1353, 1345, 1321, 1293, 1276, 1252, 1235, 1197, 1182, 1142, 1123, 1092, 1057, 1032, 1001, 981, 947, 922, 881, 865, 810, 783, 768, 753, 714, 691, 655, 622, 607 cm^{-1}.

Ethyl 4-(2-chloropyridin-3-yl)-5-hydroxy-2-methyl-1-propyl-1*H*-indole-3-carboxylate (13'b): Yellow solid (562 mg, 43%). **Mp** 72 – 74˚C; **^{1}H NMR** (400 MHz, $CDCl_3$) δ 8.40 (dd, *J* = 4.8, 2.0 Hz, 1H), 7.61 (dd, *J* = 7.5, 2.0 Hz, 1H), 7.30 (dd, *J* = 7.5, 4.8 Hz, 1H), 7.24 (d, *J* = 1.0 Hz, 1H), 6.91 (d, *J* = 8.8 Hz, 1H), 4.04 (t, *J* = 7.5 Hz, 2H), 3.86 (dq, *J* = 10.7, 7.1 Hz,

1H), 3.48 (dq, *J* = 10.8, 7.1 Hz, 1H), 2.59 (s, 3H), 1.79 (h, *J* = 7.5 Hz, 2H), 1.00 (dt, *J* = 13.7, 7.3 Hz, 6H). **^{13}C NMR** (101 MHz, $CDCl_3$) δ 165.83, 152.00, 148.51, 148.16, 144.21, 140.72, 134.02, 131.54, 124.80, 122.45, 115.01, 112.00, 111.06, 105.34, 59.92, 45.14, 23.22, 14.23, 12.14, 11.55. **HRMS** (ESI+): *m/z* calculated for $C_{20}H_{21}ClN_2O_3$ $[M+H]^+$: 373.1313, found 373.1310. **IR:** 3323, 2958, 2935, 2872, 1644, 1586, 1574, 1556, 1518, 1477, 1454, 1422, 1396, 1374, 1356, 1332, 1300, 1290, 1271, 1244, 1228, 1206, 1183, 1163, 1147, 1121, 1082, 1050, 1036, 1009, 966, 928, 903, 890, 862, 814, 790, 759, 752, 731, 701 cm^{-1}.

Ethyl 1-benzyl-6-(2-chloropyridin-3-yl)-5-hydroxy-2-methyl-1*H*-indole-3-carboxylate (13c): Yellow solid (50 mg, 11%). **Mp** 185 – 187 ˚C; **^{1}H NMR** (400 MHz, $CDCl_3$) δ 8.38 (dd, *J* = 4.8, 2.0 Hz, 1H), 7.81 (s, 1H), 7.72 (dd, *J* = 7.5, 2.0 Hz, 1H), 7.31 – 7.25 (m, 4H), 7.07 (s, 1H), 6.98 (d, *J* = 7.8 Hz, 2H), 5.32 (s, 2H), 4.40 (q, *J* = 7.1 Hz, 2H), 2.72 (s, 3H), 1.43 (t, *J* = 7.1 Hz, 3H). **^{13}C NMR** (101 MHz, $CDCl_3$) δ 166.24, 151.38, 148.84, 148.67, 146.65, 141.20, 136.21, 134.18, 131.50, 129.14, 128.44, 127.90, 126.03, 122.38, 120.72, 111.61, 107.55, 104.30, 59.85, 46.92, 14.79, 12.34. **HRMS** (ESI+): *m/z* calculated for $C_{24}H_{21}ClN_2O_3$ $[M+H]^+$: 421.1313, found 421.1307. **IR:** 3246, 2969, 2920, 2849, 1735, 1694, 1627, 1581, 1562, 1527, 1495, 1449, 1395, 1377, 1357, 1322, 1298, 1221, 1201, 1176, 1124, 1092, 1077, 1051, 1017, 1009, 989, 924, 894, 881, 868, 856, 802, 795, 777, 750, 730, 716, 695 cm^{-1}.

Ethyl 1-benzyl-4-(2-chloropyridin-3-yl)-5-hydroxy-2-methyl-1H-indole-3-carboxylate (13'c): Yellow solid (323 mg, 73%). **Mp** 83 – 85 ˚C; **^{1}H NMR** (400 MHz, $CDCl_3$) δ 8.41 (dd, *J* = 4.8, 2.0 Hz, 1H), 7.67 (dd, *J* = 7.5, 2.0 Hz, 1H), 7.34 – 7.27 (m, 4H), 7.19 (d, *J* = 8.8 Hz, 1H), 7.05 – 7.02 (m, 2H), 6.88 (d, *J* = 8.8 Hz, 1H), 5.33 (s, 2H), 3.88 (dq, *J* = 10.8, 7.1 Hz, 1H), 3.57 (dq, *J* = 10.8, 7.2 Hz, 1H), 2.58 (s, 3H), 1.05 (t, *J* = 7.1 Hz, 3H). **^{13}C NMR** (101 MHz, $CDCl_3$) δ 165.67, 152.08, 148.60, 148.42, 144.53, 140.76, 136.37, 133.70, 132.00, 129.13, 127.88, 126.15, 124.92, 122.50, 115.10, 112.33, 111.34, 106.11, 60.06, 46.96, 14.26, 12.24. **HRMS** (ESI+): *m/z* calculated for $C_{24}H_{21}ClN_2O_3$ $[M+H]^+$: 421.1313, found 421.1301. **IR:** 1681, 1605, 1573, 1562, 1523, 1496, 1463, 1434, 1421, 1393, 1371, 1332, 1299, 1270, 1226, 1205, 1180, 1153, 1122, 1084, 1054, 1028, 1016, 1003, 939, 902, 865, 797, 757, 727, 703, 647, 623, 601, 562, 523 cm^{-1}.

Ethyl 6-(2-chloropyridin-3-yl)-5-hydroxy-2-methyl-1-phenyl-1*H*-indole-3-carboxylate (13d): White solid (23 mg, 2%). **Mp** 252 – 254 ˚C; **^{1}H NMR** (400 MHz, DMSO) δ 9.40 (s, 1H), 8.36 (dd, *J* = 4.8, 2 Hz, 1H), 7.77 (dd, *J* = 7.5, 2.0 Hz, 1H), 7.66 (s, 1H), 7.66 – 7.61 (m, 2H), 7.59 – 7.54 (m, 1H), 7.51 – 7.48 (m, 2H), 7.40 (dd, *J* = 7.5, 4.8 Hz, 1H), 6.70 (s, 1H), 4.34 (q, *J* = 7.1 Hz, 2H), 2.52 (s, 3H), 1.40 (t, *J* = 7.1 Hz, 3H). **^{13}C NMR** (150 MHz, DMSO) δ 164.98, 150.47, 150.13, 148.07, 145.72, 141.05, 135.73, 134.61, 131.07, 129.95, 128.91, 127.95, 127.31, 122.73, 121.00, 111.62, 105.84, 103.52, 59.07, 14.53, 12.94. **HRMS** (ESI+): *m/z* calculated for $C_{23}H_{19}ClN_2O_3$ $[M+H]^+$: 407.1157, found 407.1159. **IR:** 3276, 3053, 3002, 2920, 2846, 1736, 1648, 1595, 1555, 1521, 1493, 1469, 1458, 1443, 1416, 1392, 1375, 1308, 1276, 1231, 1197, 1174, 1160, 1124, 1083, 1058, 1024, 1001, 991, 972, 947, 921, 892, 871, 863, 852, 809, 783, 763, 752, 720, 699, 677, 664, 651, 618, 555, 544 cm^{-1}.

Ethyl 4-(2-chloropyridin-3-yl)-5-hydroxy-2-methyl-1-phenyl-1H-indole-3-carboxylate (13'd): Yellow solid (95 mg, 8%). **Mp** 187 – 189 ˚C; **^{1}H NMR** (400 MHz, $CDCl_3$) δ 8.44 (dd, *J* = 4.8, 2.0 Hz, 1H), 7.68 (dd, *J* = 7.5, 2.0 Hz, 1H), 7.60 – 7.50 (m, 3H), 7.39 – 7.29 (m, 3H), 6.96 (d, *J* = 8.8 Hz, 1H), 6.85 (d, *J* = 8.8 Hz, 1H), 3.96 – 3.88 (m, 1H), 3.60 – 3.52 (m, 1H), 2.43 (s, 3H), 1.07 (t, *J* = 7.1 Hz, 3H). **^{13}C NMR** (101 MHz, $CDCl_3$) δ 165.65, 152.19, 148.80, 148.57, 144.84, 140.70, 136.66, 133.60, 133.40, 129.95, 129.07, 128.46, 124.63, 122.58, 114.71, 112.40, 112.33, 106.50, 60.12, 29.84, 14.29, 13.25. **HRMS** (ESI+): *m/z* calculated for $C_{23}H_{19}ClN_2O_3$$[M+H]^+$: 407.1157, found 407.1153. **IR:** 3053, 2956, 2918, 2848, 1687, 1668, 1595, 1572, 1531, 1495, 1474, 1455, 1433, 1397, 1385, 1370, 1322, 1306, 1275, 1248, 1202, 1171, 1131, 1085, 1075, 1068, 1059, 1051, 1012, 999, 963, 942, 924, 890, 871, 851, 798, 782, 769, 757, 749, 719, 707, 693, 664, 652, 631, 602, 566 cm^{1-}.

General procedures for the synthesis of cyclized adduct (14 and 15): To a solution of **13a** (189 mg, 0.57 mmol) in anhydrous DMF (2 ml) was added potassium carbonate (192 mg, 1.71 mmol) and the mixture was refluxed at 130 ºC for 2 h. After completion of the reaction, the reaction mixture was extracted with ethyl acetate. The combined organic extracts were dried over anhydrous $MgSO_4$, then filtered and concentrated under reduced pressure to give crude product. Finally, the crude product was purified by column chromatography to give the desired product.

Ethyl 2-methyl-1*H*-pyrido[3',2':4,5]furo[2,3-*f*]indole-3-carboxylate (14a): Yellow solid (140 mg, 83%). **Mp** 260 – 262 ˚C; **^{1}H NMR** (400 MHz, DMSO) *δ* 12.14 (s, 1H), 8.61 (dd, *J* = 7.5, 1.8 Hz, 1H), 8.36 (dd, *J* = 4.9, 1.7 Hz, 1H), 8.11 (d, *J* = 0.8 Hz, 1H), 8.10 (s, 1H), 7.43 (dd, *J* = 7.6, 4.9 Hz, 1H), 4.32 (q, *J* = 7.1 Hz, 2H), 2.72 (s, 3H), 1.39 (t, *J* = 7.1 Hz, 3H). **^{13}C NMR** (101 MHz, DMSO) δ 164.85, 163.02, 150.11, 147.35, 145.27, 132.04, 129.95, 127.90, 119.16, 117.32, 117.27, 103.78, 102.98, 101.54, 58.97, 14.48, 14.08. **HRMS** (ESI+): *m/z* calculated for $C_{17}H_{14}N_2O_3$ $[M+H]^+$: 295.1077, found 295.1074. **IR:** 3200, 3066, 2976, 2924, 2851, 1680, 1645, 1599, 1583, 1544, 1511, 1480, 1468, 1455, 1433, 1403, 1384, 1324, 1298, 1255, 1235, 1207, 1186, 1159, 1130, 1116, 1109, 1082, 1036, 999, 980, 922, 882, 856, 834, 811, 794, 783, 772, 755, 741, 698, 663, 622, 583 cm^{-1}.

Ethyl 2-methyl-3*H*-pyrido[3',2':4,5]furo[3,2-*e*]indole-1-carboxylate (15a): White solid (39.5 mg, 89%). **Mp** 233 – 235 ˚C; **^{1}H NMR** (400 MHz, DMSO) δ 12.24 (s, 1H), 8.92 (dd, *J* = 7.8, 1.8 Hz, 1H), 8.38 (dd, *J* = 4.8, 1.7 Hz, 1H), 7.63 (d, *J* = 8.7 Hz, 1H), 7.57 (d, *J* = 8.8 Hz, 1H), 7.46 (dd, *J* = 2, 4.8 Hz, 1H), 4.41 (q, *J* = 7.1 Hz, 2H), 2.69 (s, 3H), 1.36 (t, *J* = 7.1 Hz, 3H). **^{13}C NMR** (101 MHz, DMSO) δ 165.25, 161.99, 150.53, 144.50, 144.05, 134.76, 131.76, 120.24, 118.96, 117.30, 112.66, 112.62, 106.31, 104.98, 59.67, 14.62, 14.42. **HRMS** (ESI+): *m/z* calculated for $C_{17}H_{14}N_2O_3$ $[M+H]^+$: 295.1077, found 295.1075. **IR:** 2822, 1693, 1618, 1587, 1543, 1486, 1462, 1441, 1425, 1404, 1393, 1371, 1338, 1320, 1285, 1264, 1231, 1191, 1154, 1115, 1096, 1076, 1060, 1050, 1019, 998, 942, 932, 903, 876, 865, 854, 797, 773, 754, 662, 642, 628, 580, 547 cm^{-1}.

Ethyl 2-methyl-1-propyl-1*H*-pyrido[3',2':4,5]furo[2,3-*f*]indole-3-carboxylate (14b): White solid (58.7 mg, 81%). **Mp** 138 – 140 ˚C; **^{1}H NMR** (400 MHz, DMSO) δ 8.53 (dd, *J* = 7.5, 1.7 Hz, 1H), 8.37 (dd, *J* = 4.9, 1.7 Hz, 1H), 8.32 (d, *J* = 0.8 Hz, 1H), 8.11 (d, *J* = 0.7 Hz, 1H), 7.43 (dd, *J* = 7.5, 5 Hz, 1H), 4.33 (q, *J* = 7.1 Hz, 2H), 4.24 (t, *J* = 7.4 Hz, 2H), 2.77 (s, 3H), 1.78 (h, *J* = 7.4 Hz, 2H), 1.40 (t, *J* = 7.1 Hz, 3H), 0.94 (t, *J* = 7.4 Hz, 3H). **^{13}C NMR** (101 MHz, DMSO) δ 164.70, 163.05, 150.20, 147.36, 145.31, 133.00, 129.68, 126.97, 119.16, 117.38, 117.22, 102.93, 101.72, 59.01, 22.33, 14.39, 11.88, 10.98. **HRMS** (ESI+): *m/z* calculated for $C_{20}H_{20}N_2O_3$ $[M+H]^+$: 337.1547, found 337.1542. **IR:** 3021, 2978, 2930, 2905, 2879, 1690, 1638, 1592, 1531, 1499, 1478, 1467, 1452, 1442, 1402, 1377, 1367, 1345, 1315, 1285, 1250, 1231, 1208, 1177, 1156, 1136, 1124, 1098, 1058, 1018, 998, 947, 914, 890, 870, 857, 834, 814, 799, 773, 742, 729, 700, 684, 661 cm^{-1}.

Ethyl 2-methyl-3-propyl-3*H*-pyrido[3',2':4,5]furo[3,2-*e*]indole-1-carboxylate (15b): Yellow solid (38.5 mg, 85%). **Mp** 104 – 106 ˚C; **^{1}H NMR** (400 MHz, DMSO) δ 8.66 (dd, *J* = 7.9, 1.7 Hz, 1H), 8.38 (dd, *J* = 4.9, 1.7 Hz, 1H), 7.81 (d, *J* = 8.9 Hz, 1H), 7.61 (d, *J* = 9.0 Hz, 1H), 7.46 (dd, *J* = 7.8, 4.8 Hz, 1H), 4.43 (q, *J* = 7.1 Hz, 2H), 4.26 (t, *J* = 7.5 Hz, 2H), 2.70 (s, 3H), 1.72 (h, *J* = 7.4 Hz, 2H), 1.35 (t, *J* = 7.1 Hz, 3H), 0.90 (t, *J* = 7.4 Hz, 3H). **^{13}C NMR** (101 MHz, DMSO) δ 165.35, 162.07, 150.66, 144.60, 143.60, 134.55, 132.54, 119.57, 118.96, 117.11, 112.58, 111.66, 106.24, 105.19, 59.94, 44.61, 22.67, 14.36, 12.14, 10.98. **HRMS** (ESI+): *m/z* calculated for $C_{20}H_{20}N_2O_3$ $[M+H]^+$: 337.1547, found 337.1544. **IR:** 2951, 2924, 2872, 2851, 1683, 1605, 1580, 1511, 1464, 1431, 1401, 1386, 1378, 1342, 1295, 1261, 1235, 1192, 1171, 1150, 1119, 1091, 1066, 1052, 1036, 1016, 969, 913, 898, 878, 859, 806, 796, 776, 749, 731, 659 cm^{-1}.

Ethyl 1-benzyl-2-methyl-1*H*-pyrido[3',2':4,5]furo[2,3-*f*]indole-3-carboxylate (14c): Yellow solid (26 mg, 57%). **Mp** 178 – 180 ˚C; **^{1}H NMR** (400 MHz, DMSO) δ 8.50 (dd, *J* = 7.5, 1.7 Hz, 1H), 8.37 (d, *J* = 5 Hz, 2H),

8.20 (s, 1H), 7.43 (dd, *J* = 7.5, 5 Hz, 1H), 7.35 – 7.30 (m, 2H), 7.25 (t, *J* = 6.9 Hz, 1H), 7.06 (d, *J* = 7.3 Hz, 2H), 5.65 (s, 2H), 4.36 (q, *J* = 7.1 Hz, 2H), 2.74 (s, 3H), 1.41 (t, *J* = 7.1 Hz, 3H). **^{13}C NMR** (101 MHz, DMSO) δ 164.68, 163.07, 150.37, 147.63, 145.52, 136.78, 133.54, 129.79, 128.80, 127.38, 126.99, 126.02, 119.25, 117.73, 117.05, 103.65, 103.07, 101.99, 59.20, 14.39, 12.06. **HRMS** (ESI+): *m/z* calculated for $C_{24}H_{20}N_2O_3$ $[M+H]^+$: 385.1547, found 385.1541. **IR:** 3059, 2976, 2935, 1716, 1681, 1638, 1591, 1535, 1497, 1449, 1413, 1358, 1345, 1323, 1300, 1258, 1228, 1210, 1188, 1175, 1137, 1121, 1099, 1076, 1058, 1030, 1008, 1001, 970, 927, 907, 889, 872, 856, 815, 795, 785, 775, 760, 731, 696, 662 cm^{-1}.

Ethyl 1-benzyl-2-methyl-1*H*-pyrido[3',2':4,5]furo[2,3-*g*]indole-3-carboxylate (15c): Yellow solid (120 mg, 94%). **Mp** 141 – 143 °C; **^{1}H NMR** (400 MHz, DMSO) δ 8.69 (dd, *J* = 7.9, 1.8 Hz, 1H), 8.39 (dd, *J* = 4.8, 1.7 Hz, 1H), 7.74 (d, *J* = 9.0 Hz, 1H), 7.58 (d, *J* = 8.9 Hz, 1H), 7.45 (dd, *J* = 7.9, 4.8 Hz, 1H), 7.30 – 7.20 (m, 3H), 7.01 (d, *J* = 6.8 Hz, 2H), 5.60 (s, 2H), 4.43 (q, *J* = 7.1 Hz, 2H), 2.66 (s, 3H), 1.34 (t, *J* = 7.3 Hz, 3H). **^{13}C NMR** (101 MHz, DMSO) δ 165.27, 162.08, 150.75, 144.68, 143.83, 136.91, 134.56, 132.90, 128.75, 127.35, 126.04, 119.66, 118.96, 117.01, 112.71, 111.73, 106.57, 105.78, 60.03, 14.27, 12.27. **HRMS** (ESI+): *m/z* calculated for $C_{24}H_{20}N_2O_3$ $[M+H]^+$: 385.1547, found 385.1540. **IR:** 3085, 3060, 2962, 2900, 1676, 1604, 1585, 1514, 1496, 1467, 1455, 1431, 1402, 1388, 1378, 1352, 1341, 1301, 1262, 1232, 1195, 1171, 1144, 1122, 1095, 1063, 1053, 1041, 1021, 1005, 974, 948, 907, 895, 858, 847, 805, 800, 776, 753, 743, 733, 695, 660, 650, 622 cm^{-1}.

Ethyl 2-methyl-1-phenyl-1*H*-pyrido[3',2':4,5]furo[2,3-*f*]indole-3-carboxylate (14d): Yellow solid (7 mg, 32%). **Mp** 120 – 122 °C; **^{1}H NMR** (400 MHz, $CDCl_3$) δ 8.39 – 8.37 (m, 2H), 8.11 (dd, *J* = 7.5, 1.7 Hz, 1H), 7.68 – 7.60 (m, 3H), 7.46 (s, 1H), 7.24 – 7.39 (m, 2H), 7.24 (dd, *J* = 7.6, 5 Hz, 1H), 4.49 (q, *J* = 7.1 Hz, 2H), 2.65 (s, 3H), 1.53 (t, *J* = 7.1 Hz, 3H). **^{13}C NMR** (150 MHz, $CDCl_3$) δ 166.02, 164.01, 151.67, 147.89, 145.73, 136.62, 135.27, 130.19, 129.36, 128.95, 128.55, 127.64, 118.71, 118.61, 117.87, 105.57, 103.51, 102.30, 59.99, 14.84, 13.51. **HRMS** (ESI+): *m/z* calculated for $C_{23}H_{18}N_2O_3$ $[M+H]^+$: 371.1390, found 371.1389. **IR:** 3055, 2978, 2958, 2922, 1687, 1594, 1580, 1556, 1498, 1415, 1372, 1347, 1327, 1313, 1273, 1259, 1249, 1234, 1217, 1187, 1172, 1152, 1113, 1094, 1071, 1061, 1047, 1032, 1022, 1011, 1000, 974, 961, 925, 907, 872, 859, 844, 834, 808, 802, 794, 772, 763, 752, 720, 710, 695, 662, 647 cm^{-1}.

Ethyl 2-methyl-1-phenyl-1*H*-pyrido[3',2':4,5]furo[2,3-*g*]indole-3-carboxylate (15d): Orange solid (45 mg, 35%). **Mp** 115 – 117 °C; **^{1}H NMR** (400 MHz, $CDCl_3$) δ 8.82 (dd, *J* = 7.8, 1.7 Hz, 1H), 8.41 (dd, *J* = 4.9, 1.8 Hz, 1H), 7.63 – 7.55 (m, 3H), 7.45 (d, *J* = 8.8 Hz, 1H), 7.39 – 7.33 (m, 3H), 7.11 (d, *J* = 8.9 Hz, 1H), 4.56 (q, *J* = 7.1 Hz, 2H), 2.56 (s, 3H), 1.46 (t, *J* = 7.1 Hz, 3H). **^{13}C NMR** (101 MHz, $CDCl_3$) δ 166.33, 163.01, 151.97, 144.89, 144.85, 143.92, 136.67, 135.04, 134.89, 130.07, 129.40, 128.61, 120.30, 118.88, 118.09, 113.84, 111.56, 107.41, 107.17, 60.59, 14.75, 13.76. **HRMS** (ESI+): *m/z* calculated for $C_{23}H_{18}N_2O_3$ $[M+H]^+$: 371.1390, found 371.1383. **IR:** 3056, 2980, 2957, 2923, 2850, 1690, 1596, 1580, 1499, 1453, 1415, 1400, 1382, 1373, 1349, 1327, 1317, 1261, 1235, 1217, 1187, 1172, 1151, 1115, 1094, 1071, 1060, 1047, 1032, 1022, 1011, 1000, 961, 925, 907, 871, 860, 845, 802, 795, 772, 762, 752, 720, 695, 669, 660, 649, 633 cm^{-1}.

Spectroscopic Characterisation: Solutions were prepared in commercially available solvents (spectroscopic or liquid chromatography grade), such as acetonitrile (ACN) and toluene, and directly used in experiments without further purification. The UV-visible absorption spectra of dilute solutions were recorded using a Perkin Elmer Lambda 950 spectrophotometer with a blank correction. Emission spectra, excitation spectra and photoluminescence quantum yield (ϕ) were recorded using a double grating Horiba Fluorolog 3-22 spectrofluorometer with cooled PMT, with corrections for both excitation and emission wavelength dependent response of the system and zero counts. Absolute quantum yields were determined using the 10 cm spectralon integrating sphere accessory. On all sample solutions a 0.1% neutral density filter was used for measuring the Raleigh scatter.

DFT calculations: The ground state geometries of synthesized compound **15a, 14b, 15b, 14c and 15c** were optimized using density functional theory calculations with B3LYP functional and 6-31+G(d,p) basis using Gaussian 09. RevD.01 software package.[58] For all the geometries, vibrational frequencies were calculated to ascertain the optimized geometries at stationary point. While optimization, polarized continuum model (PCM) based solvation for Acetonitrile and Toluene solvents was used. Further, time-dependent DFT (TD-DFT) calculations were performed to calculate vertical excitation with linear response in acetonitrile and toluene solvent environment for each molecule to validate λ_{max} obtained from UV-Vis absorption. Further, the predicted excited state geometries were completely relaxed, without symmetry, to calculate λ_{max} for emission and to compare with the fluorescence emission spectra.

Acknowledgements

We thank the KU Leuven for financial support (Project C14/19/78). RS thanks IIT (ISM) Dhanbad for a graduate fellowship. We acknowledge financial support from the Research Foundation - Flanders through a postdoctoral fellowship to E.D. (FWO Grant Number 12O3719N) and a bilateral grant (G0F6619N), and the ERC through the Marie Curie ITN iSwitch PhD fellowship to H.B. (Grant Number 642196). R.S. and H.B. thank Giacomo Romolini and Bjorn Dieu from the Molecular Imaging and Photonics lab KU Leuven for helpful discussions. Mass spectrometry was made possible by the support of the Hercules Foundation of the Flemish Government (grant 20100225-7).

Keywords: 5-Hydroxyindoles • enamines • Nenitzescu reaction • nucleophilic aromatic substitution • polycyclic heterocycles • pyrido (furo) indoles • quinones

[1] F. de Sa Alves, E. Barreiro, C. Manssour Fraga, *Mini-Reviews Med. Chem.* **2009**, *9*, 782–793.

[2] D. A. Horton, G. T. Bourne, M. L. Smythe, *Chem. Rev.* **2003**, *103*, 893–930.

[3] C. Duarte, E. Barreiro, C. Fraga, *Mini-Reviews Med. Chem.* **2007**, *7*, 1108–1119.

[4] R. Singh, R. Prakash, W. Dehaen, in *Adv. Heterocycl. Chem.*, Elsevier Inc., **2021**, pp. 319–410.

[5] G. R. Allen, in *Org. React.*, John Wiley & Sons, Inc., Hoboken, NJ, USA, **2011**, pp. 337–454.

[6] S. Patil, R. Patil, D. Miller, *Curr. Org. Chem.* **2008**, *12*, 691–717.

[7] F. Dumitrascu, M. A. Ilies, in *Adv. Heterocycl. Chem.*, Elsevier Inc., **2021**, pp. 65–157.

[8] J. Mei, N. L. C. Leung, R. T. K. Kwok, J. W. Y. Lam, B. Z. Tang, *Chem. Rev.* **2015**, *115*, 11718–11940.

[9] H. Ito, K. Ozaki, K. Itami, *Angew. Chemie Int. Ed.* **2017**, *56*, 11144–11164.

[10] D. A. Erlanson, S. W. Fesik, R. E. Hubbard, W. Jahnke, H. Jhoti, *Nat. Rev. Drug Discov.* **2016**, *15*, 605–619.

[11] T. V. Sravanthi, S. L. Manju, *Eur. J. Pharm. Sci.* **2016**, *91*, 1–10.

[12] N. Kaushik, N. Kaushik, P. Attri, N. Kumar, C. Kim, A. Verma, E. Choi, *Molecules* **2013**, *18*, 6620–6662.

[13] J. T. Erickson, *Exp. Neurol.* **2020**, *326*, 113162.

[14] G. Wang, L. Geng, *Anal. Chem.* **2005**, *77*, 20–29.

[15] H. Vigerelli, J. M. Sciani, P. M. C. Pereira, A. A. Lavezo, A. C. R. Silva, R. C. O. Collaço, T. Rocha, T. C. Bueno, D. C. Pimenta, *J. Venom. Anim. Toxins Incl. Trop. Dis.* **2020**, *26*, DOI 10.1590/1678-

9199-jvatitd-2019-0050.

[16] A. J. Kochanowska-Karamyan, M. T. Hamann, *Chem. Rev.* **2010**, *110*, 4489–4497.

[17] M. R. Herod, O. O. Adeyemi, J. Ward, K. Bentley, M. Harris, N. J. Stonehouse, S. J. Polyak, *J. Gen. Virol.* **2019**, *100*, 1293–1302.

[18] I. A. Leneva, R. J. Russell, Y. S. Boriskin, A. J. Hay, *Antiviral Res.* **2009**, *81*, 132–140.

[19] Q. Zhang, F. Zhang, Y. Chen, Y. Dou, H. Tao, D. Zhang, R. Wang, X. Li, J. Zhang, *Chem. Mater.* **2017**, *29*, 8221–8238.

[20] G. Fronza, A. Mele, E. Redenti, P. Ventura, *J. Org. Chem.* **1996**, *61*, 909–914.

[21] G. Van Baelen, S. Hostyn, L. Dhooghe, P. Tapolcsányi, P. Mátyus, G. Lemière, R. Dommisse, M. Kaiser, R. Brun, P. Cos, L. Maes, G. Hajós, Z. Riedl, I. Nagy, B. U. W. Maes, L. Pieters, *Bioorg. Med. Chem.* **2009**, *17*, 7209–7217.

[22] T. K. Mazu, J. R. Etukala, M. R. Jacob, S. I. Khan, L. A. Walker, S. Y. Ablordeppey, *Eur. J. Med. Chem.* **2011**, *46*, 2378–2385.

[23] S. U. Dighe, S. Khan, I. Soni, P. Jain, S. Shukla, R. Yadav, P. Sen, S. M. Meeran, S. Batra, *J. Med. Chem.* **2015**, *58*, 3485–3499.

[24] Y.-C. Kong, K.-F. Cheng, R. C. Cambie, P. G. Waterman, *J. Chem. Soc. Chem. Commun.* **1985**, 47.

[25] R. E. Moore, C. Cheuk, X. Q. G. Yang, G. M. L. Patterson, R. Bonjouklian, T. A. Smitka, J. S. Mynderse, R. S. Foster, N. D. Jones, J. K. Swartzendruber, J. B. Deeter, *J. Org. Chem.* **1987**, *52*, 1036–1043.

[26] A. Park, R. E. Moore, G. M. . Patterson, *Tetrahedron Lett.* **1992**, *33*, 3257–3260.

[27] M. Sanchez, O. B. Mcmanus, *Neuropharmacology* **1996**, *35*, 963–968.

[28] K. Brachwitz, A. Hilgeroth, *Bioorg. Med. Chem. Lett.* **2002**, *12*, 411–413.

[29] M. Krug, B. Voigt, C. Baumert, R. Lüpken, J. Molnár, A. Hilgeroth, *Eur. J. Med. Chem.* **2010**, *45*, 2683–2688.

[30] L. W. Deady, A. J. Kaye, G. J. Finlay, B. C. Baguley, W. A. Denny, *J. Med. Chem.* **1997**, *40*, 2040–2046.

[31] I. A. Khan, M. V Kulkarni, M. Gopal, M. S. Shahabuddin, C.-M. Sun, *Bioorg. Med. Chem. Lett.* **2005**, *15*, 3584–3587.

[32] M. Osswald, D. Dorsch, W. Mederski, C. Wilm, C. Schmitges, M. Christadler, *Endothelin Receptor Antagonists EP0755934A1*, **1997**.

[33] B. Voigt, M. Krug, C. Schächtele, F. Totzke, A. Hilgeroth, *ChemMedChem* **2008**, *3*, 120–126.

[34] V. Tell, K. A. Mahmoud, K. Wichapong, C. Schächtele, F. Totzke, W. Sippl, A. Hilgeroth, *Medchemcomm* **2012**, *3*, 1413.

[35] G. Balasubramanian, S. Narayanan, L. Andiappan, T. Sappanimuthu, S. Thirunavukkarasu, S. Sundaram, S. Natarajan, N. Sivaraman, S. Rajagopal, F. A. A. Nazumudeen, S. Saxena, S. L. Vishwakarma, S. Narayanan, G. V. R. Sharma, C. V. Srinivasan, N. Kilambi, *Bioorg. Med. Chem.* **2016**, *24*, 5702–5716.

[36] J. Luzzio, Michael, M. Besterman, Jeffrey, G. Evans, Michael, R. Johnson, M., M. Dezube, J. Profeta, Salvatore, *Cyclic Antitumor Compounds WO 92/21661*, **1992**.

[37] F. P. Robinson, R. K. Brown, *Can. J. Chem.* **1964**, *42*, 1940–1947.

[38] R. Dalpozzo, G. Bartoli, *Curr. Org. Chem.* **2005**, *9*, 163–178.

[39] A. D. Batcho, W. Leimgruber, *Org. Synth.* **1985**, *63*, 214.

[40] M. Anwar, S. Yang, W. Xu, J. Liu, S. Perveen, X. Kong, S. T. Zehra, X. Fang, *Commun. Chem.* **2019**, *2*, 85.

[41] W. S. Yue, J. J. Li, *Org. Lett.* **2002**, *4*, 2201–2203.

[42] J. Liu, A. E. Fitzgerald, N. S. Mani, *J. Org. Chem.* **2008**, *73*, 2951–2954.

[43] V. Iaroshenko, U. Groth, N. Kryvokhyzha, S. Obeid, A. Tolmachev, T. Wesch, *Synlett* **2008**, *2008*, 343–346.

[44] M. Funicello, V. Laboragine, R. Pandolfo, P. Spagnolo, *Synlett* **2010**, *2010*, 77–80.

[45] W. Sun, M. Wang, Y. Zhang, L. Wang, *Org. Lett.* **2015**, *17*, 426–429.

[46] M. G. Ciulla, S. Zimmermann, K. Kumar, *Org. Biomol. Chem.* **2019**, *17*, 413–431.

[47] M. Anwar, S. Yang, W. Xu, J. Liu, S. Perveen, X. Kong, S. T. Zehra, X. Fang, *Commun. Chem.* **2019**, *2*, 85.

[48] C.-C. Xie, R. Tan, Y.-K. Liu, *Org. Chem. Front.* **2019**, *6*, 919–924.

[49] N. Chernyak, D. Tilly, Z. Li, V. Gevorgyan, *Chem. Commun.* **2010**, *46*, 150–152.

[50] C. Liu, G. Wang, Y. Wang, K. Van Hecke, O. P. Pereshivko, V. A. Peshkov, *Tetrahedron Lett.* **2018**, *59*, 1823–1827.

[51] V. O. Iaroshenko, A. Gevorgyan, S. Mkrtchyan, T. Grigoryan, E. Movsisyan, A. Villinger, P. Langer, *ChemCatChem* **2015**, *7*, 316–324.

[52] R. Singh, T. Horsten, R. Prakash, S. Dey, W. Dehaen, *Beilstein J. Org. Chem.* **2021**, *17*, 977–982.

[53] G. Domschke, *Zeitschrift für Chemie* **2010**, *6*, 41–51.

[54] P. Xu, K. Huang, Z. Liu, M. Zhou, W. Zeng, *Tetrahedron Lett.* **2013**, *54*, 2929–2933.

[55] V. S. Velezheva, A. I. Sokolov, A. G. Kornienko, K. A. Lyssenko, Y. V. Nelyubina, I. A. Godovikov, A. S. Peregudov, A. F. Mironov, *Tetrahedron Lett.* **2008**, *49*, 7106–7109.

[56] W. Zhang, J. Kong, D. Hu, M. Tao, X. Niu, S. Vdović, D. Aumiler, Y. Ma, A. Xia, *J. Phys. Chem. C* **2020**, *124*, 5574–5582.

[57] G. He, L. L. Zhou, H. Song, Z. Kuang, X. Wang, Q. Guo, H. Y. Lu, A. Xia, *Phys. Chem. Chem. Phys.* **2018**, *20*, 7514–7522.

[58] M. J. Frisch, G. W. Trucks, H. B. Schlegel, G. E. Scuseria, M. A. Robb, J. R. Cheeseman, G. Scalmani, V. Barone, B. Mennucci, G. A. Petersson, H. Nakatsuji, M. Caricato, X. Li, H. P. Hratchian, A. F. Izmaylov, J. Bloino, G. Zheng, J. L. Sonnenberg, M. Hada, M. Ehara, K. Toyota, R. Fukuda, J. Hasegawa, M. Ishida, T. Nakajima, Y. Honda, O. Kitao, H. Nakai, T. Vreven, J. A. Montgomery Jr., J. E. Peralta, F. Ogliaro, M. Bearpark, J. J. Heyd, E. Brothers, K. N. Kudin, V. N. Staroverov, R. Kobayashi, J. Normand, K. Raghavachari, A. Rendell, J. C. Burant, S. S. Iyengar, J. Tomasi, M. Cossi, N. Rega, J. M. Millam, M. Klene, J. E. Knox, J. B. Cross, V. Bakken, C. Adamo, J. Jaramillo, R. Gomperts, R. E. Stratmann, O. Yazyev, A. J. Austin, R. Cammi, C. Pomelli, J. W. Ochterski, R. L. Martin, K. Morokuma, V. G. Zakrzewski, G. A. Voth, P. Salvador, J. J. Dannenberg, S. Dapprich, A. D. Daniels, Ö. Farkas, J. B. Foresman, J. V Ortiz, J. Cioslowski, D. J. Fox, **2009**, Gaussian 09 Revision D.01.

Entry for the Table of Contents

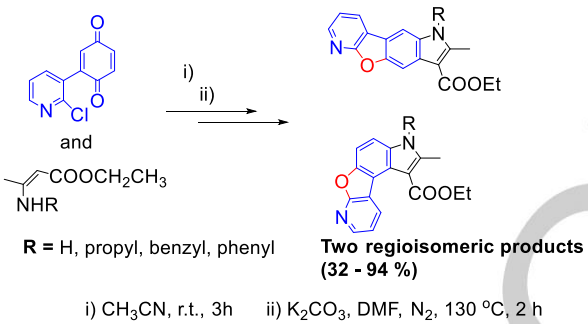

Two regioisomeric sets of 5-hydroxy indoles, prepared from Nenitzescu reaction, were transformed to polyfused ring system bearing pyridine, furan and additionally indole as key component through intramolecular nucleophilic substitution. This methodology provides simple access to various linear and angular-shaped pyrido (furo) fused indole frameworks from easily available precursors under mild reaction conditions.